LETTERS

Asymmetric diffusion as a key mechanism in Ni/Al energetic multilayer processing: A first principles study

M. Petrantoni,[a)] A. Hemeryck,[b)] J. M. Ducéré,[c)] A. Estève,[d)] C. Rossi,[e)] M. Djafari Rouhani,[f)] D. Estève,[g)] and G. Landa[h)]
Laboratoire d'Analyse et d'Architecture des Systèmes-CNRS, University of Toulouse, 7 Avenue du Colonel Roche, 31077 Toulouse, France

(Received 28 June 2010; accepted 31 August 2010; published 12 October 2010)

Adsorption and penetration of Al and Ni atoms into Ni(111) and Al(111), respectively, are investigated through first principles calculations, shedding light into the driving forces impacting Al/Ni interfaces produced during multilayer deposition. The authors show that Ni deposition follows an exothermic path toward penetration associated with small activation barriers while Al on Ni(111) path is endothermic accompanied with high activations. Moreover, Ni and Al penetrations proceed through interstitial and substitutional sites, respectively. These differentiated behaviors at early deposition stages illustrate that dual processing conditions are required to achieve the growth of specific Ni/Al interfaces during multilayer deposition processes and that a local melting process at the interface is mandatory to arrive at the formation of a proper barrier layer. © *2010 American Vacuum Society.* [DOI: 10.1116/1.3491182]

I. INTRODUCTION

Nanotechnologies are expected to open up a route to produce energetic materials with a precise control of the layers and interface structures on a chip, targeting their specific and exalted properties. In this trend, nanoenergetics-on-a-chip (NOC) technology[1] is motivating considerable effort to implement new targeted energetic functionalities into current nanosystems in order to produce tunable mechanical energy or thermal energy, or to deliver chemical species.[2] Among current NOC technologies, physical vapor deposition (PVD) is the most versatile process for the collective fabrication of multilayered films, with thicknesses in the range of tens of nanometers to 1 μm.[3–5] It has been experimentally demonstrated that the layer thicknesses and interface compositions are of importance for the energy dissipation characteristics. For example, A1/Ni multilayers with nanoscale layering are known to exhibit a rapid combustion reaction.[3] However, little is known about the interface structures and their spatial extension, and on the atomistic mechanisms generating these interfaces during the technology process. From a modeling point of view, the literature only concentrated on the simulation of combustion and initiation through empirical continuous models,[3] or using molecular dynamics methodologies on more or less "hand-built" model-systems.[6–8] However, to fully exploit the potentialities of NOC, it is crucial to understand interactions between the atoms that will form the interfaces during the technology process in order to control its stability, sensitivity, thermal energy content, and reactivity in the second stage. For this purpose, we investigate in this article, the diffusion characteristics of a metallic atom in a substrate made of a different material. The case of Ni/Al is chosen because it is a representative among bimetallic energetic materials. Focusing on the PVD process, we successively examine the behavior of a Ni atom deposited on an Al(111) surface and that of an Al atom deposited on a Ni(111) surface. The model used here represents well the first stages of the deposition where only isolated adatoms are present on the surface. To the best of our knowledge, for what concerns energetic bimetallic systems only, the adsorption, surface diffusion, and first subsurface layer incorporation restricted to substitutional sites have been reported for both Ni/Al(100) and Al/Ni(100) surfaces.[9] In the following, we calculated the reaction pathways for the adsorption and the further penetration of Ni and Al atoms on (111) Ni and Al surfaces, up to the second subsurface layer. For the diffusing atom, final substitutional as well as interstitial positions have been considered. In this qualitative approach to shed light into the basics of the interface formation, surface diffusion is neglected to be less discriminative than penetration. These mechanisms are expected to shed light into some fundamental aspects of Al/Ni multilayer deposition.

II. MATERIALS AND METHODS

First principles calculations are performed in the frame of density functional theory (DFT), using Vienna *ab initio*

[a)]Author to whom correspondence should be addressed; electronic mail: mpetrant@laas.fr
[b)]Electronic mail: ahemeryc@laas.fr
[c)]Electronic mail: jmducere@laas.fr
[d)]Electronic mail: aesteve@laas.fr
[e)]Electronic mail: rossi@laas.fr
[f)]Electronic mail: djafari@laas.fr
[g)]Electronic mail: esteve@laas.fr
[h)]Electronic mail: georges.landa@laas.fr

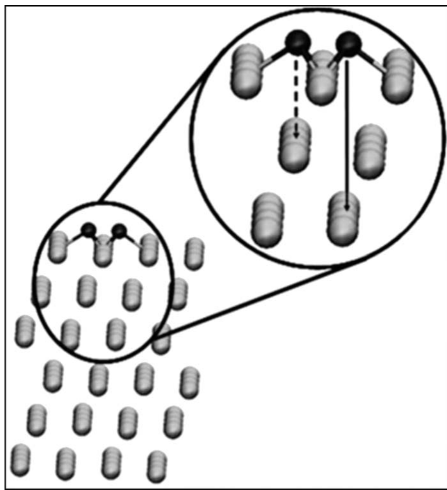

FIG. 1. Side view of the periodic Ni(111) or Al (111) supercell: six layers of 16 metallic atoms in light gray, and fcc and hexagonal adsorption sites in dark gray. Continuous and dashed lines show the difference between these sites with respect to the subsurface layers.

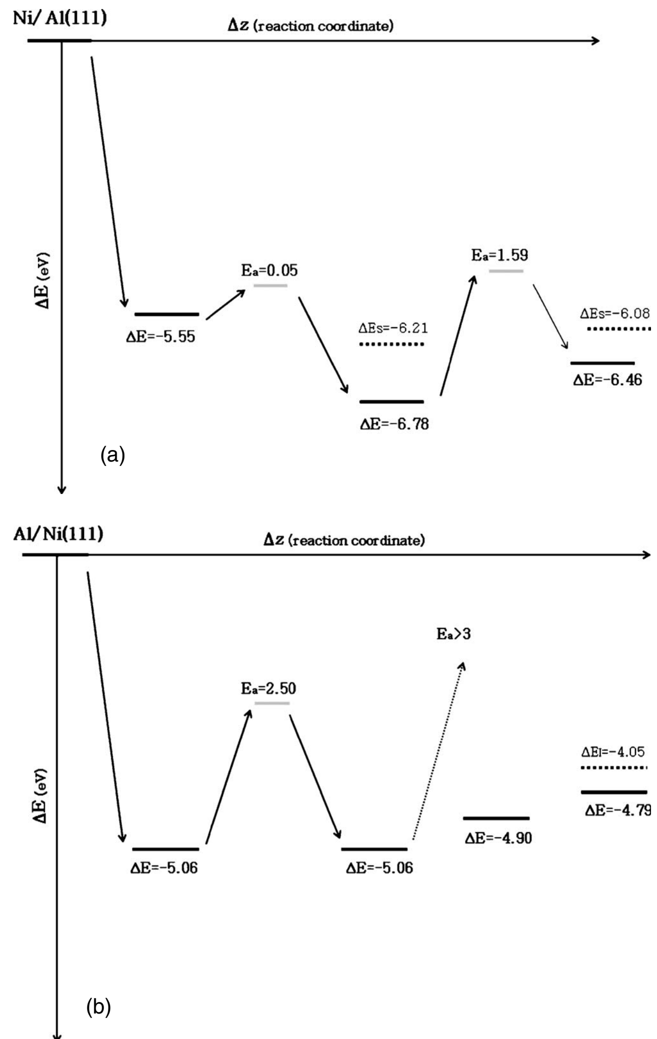

FIG. 2. Schematic reaction pathways of (a) Ni atom adsorption and penetration into Al(111), and (b) Al atom adsorption and penetration into Ni(111). Dashed lines represent the metastable substitutional and international configurations, noted E_S and E_I, respectively.

simulation (VASP) package.[10] In these calculations, the local density approximation has been associated with ultrasoft pseudopotentials of the Vanderbilt type for describing ions.[11] The substrate has been modeled by a slab made of six layers of 16 atoms each, representing the (111) surface of a fcc lattice. This slab has been extended by a 10 Å vacuum on its top, in order to build the supercell (see Fig. 1). Periodic boundary conditions have then been applied to the supercell in all three directions of the space. The slab thickness is chosen to mimic the bulk behavior. The bottom layer of the slab is therefore kept fixed during relaxations. A cut off energy of 242 eV and a $2\times2\times1$ Monkhorst–Pack mesh of k-points[12] have been adopted.

To determine the transition states, corresponding to total energy saddle points, we used a drag method. Here, at each calculation step, the z-coordinate of the adsorbed atom, normal to the surface, is kept fixed while minimizing the total energy of the system with respect to all remaining coordinates. Once the transition point is reached, full energy minimization procedure is applied again to bring the system to another local minimum.

Two different systems are investigated: Ni/Al(111) and Al/Ni(111) with fcc lattice parameters of 3.98 and 3.42 Å, respectively. Considering the symmetries of the (111) face of the fcc lattice, two different sites, represented in Fig. 1, may be assigned to the adsorbed atom: (i) an epitaxial site allowing to build a new (111) layer of the fcc lattice and (ii) a nonlattice site allowing to build a stacking fault on top of the substrate surface. In the following, these sites have been referred to as fcc site and hexagonal site, respectively.

III. DISCUSSION

The adsorption and further incorporation of a Ni atom on the Al(111) is considered first. The reaction pathway is shown in Fig. 2(a). Starting with the Ni atom far from the surface, the total energy minimization leads to Ni atom adsorbed in a hexagonal site, whatever lateral initial position. In this first minimum position, the Ni atom is almost at the same height as the Al atoms on the Al(111) substrate. This is due to the additional interaction with an atom of the first subsurface layer that is displaced during energy minimization (see Fig. 1, dashed line), pointing toward the upper hexagonal site. This first part of the pathway is highly exothermic, with a gain of 5.55 eV. Considering now the subsequent subsurface penetration of Ni atom, we first find an energy barrier of 0.05 eV before the stabilization of the Ni atom underneath the Al surface layer. In this process, an Al atom is rejected from its lattice site to the outer surface to form a dumbbell-like structure with the Ni atom. This structure further increases the energetic stability by 1.23 eV compared to the initial adsorption hexagonal site. Continuing the penetration path, the Ni atom encounters a second higher energy barrier of 1.59 eV. In its third stable minimum, between the first and second subsurface layers, the Ni atom is located in an interstitial position with the Al crystalline structure swelling around the

Ni atom. Although very close to the surface, this interstitial configuration is structurally similar to that of a Ni interstitial atom in bulk Al. Therefore, we can conclude that bulk characteristics are rapidly reached in Ni/Al structures. This last part of the reaction path is endothermic, with a loss in energy of 0.32 eV. Several other local arrangements have been tested in order to find a more stable configuration. Particularly, we tested substitutional sites for the Ni atom into the first and second subsurface layers, respectively. During this process, the Al atom, which is replaced by a Ni atom, is brought to the surface. The resulting energies are systematically higher than that of the Ni atom as interstitial, 0.57 and 0.38 eV higher than that of Ni interstitial in the first and the second subsurface layer, respectively [see SI and S2 in Fig. 2(a)].

Given its large energy barrier of 1.59 eV, the penetration of Ni atom into the second subsurface layer of Al(111) is kinetically activated at temperatures much higher than the Al melting temperature (note that the melting temperature of bulk Al is in the range of 660 °C). We believe that this transition, inhibited in the Al solid phase, requires a prior melting of Al, at least locally. Therefore, this local melting and recrystallization process, promoted by temperature and a surface/interface topography, potentially atomically defective, can be accompanied by a phase transformation from fcc Al to bcc Ni/Al, which will stabilize the reaction. On the contrary, due to the DFT calculated values, low temperature intermixing is normally limited to the first subsurface layer.

We then consider the Al adsorption and penetration into the Ni(111) surface. The associated energy diagram is shown in Fig. 2(b). The adsorption is exothermic, as in the previous case, with a comparable gain of 5.06 eV. However, the position of the adsorbed Al on top of the Ni(111) surface is somehow different. The adsorption site is far above the surface, at 1.78 Å, in a fcc site, while the hexagonal site becomes unstable. For further penetration of Al atom into subsurface layers, structures and energies show dramatic changes. The first calculated energy barrier is of 2.5 eV, drastically different from the quasibarrierless pathway for Ni penetration into Al. Overcoming this substantial barrier leads to the incorporation of the Al atom into the Ni(l11) surface layer in a substitutional position. A Ni atom is displaced on the outer surface, at 0.85 Å height. The Al atom has still not penetrated into the Ni but remains on the surface. The overall energy gain for this incorporation is zero. From this position, further penetration toward the subsurface layers, using a drag method, failed to arrive at a reasonable stable configuration. A rough estimation of this pathway shows that the activation energy should be higher than 3 eV. In the absence of a reliable reaction pathway, we calculated total energies of the systems where the Al atom is directly placed in substitutional or interstitial positions. We observe that substitutional sites are metastable. The penetration reactions are endothermic with energy losses of 0.16–0.27 eV for Al insertion into the first and second subsurface layers, respectively [see Fig. 2(b)]. Interstitial positions are all unstable in the first and second subsurface layers. They tend, after energy minimization, to a substitutional Al site. Deeper into the bulk, between the second and the third Ni(l11) subsurface layers, an Al in interstitial configuration may be stabilized. However, this configuration is not energetically favorable and shows an excess energy of 0.74 eV with respect to the sustitutional Al [see Fig. 2(b), dashed line].

IV. CONCLUSION

In conclusion, based on our DFT calculations, we show that Ni penetration into Al(111) layers follows an exothermic reaction path associated with small activation barriers, but is limited to the first subsurface layer at low temperatures. In contrast, Al penetration path into Ni(111) not only shows high activation barriers, but is also endothermic—inhibiting completely the intermixing. Also the penetration mode is different via interstitial positions for the penetration of Ni atoms into Al, while mediated by substitutional sites for the Al atoms penetrating into Ni, keeping in mind that in this last case, the activation energy required for penetration is high and unreachable under normal processing conditions. Therefore, we can conclude that an efficient intermixing can only occur at high temperatures and follows a prior melting step and phase transformation of the films. Our results also indicate that, in the absence of any contrasted processing conditions for Al and Ni deposition, respectively, the fabrication of equivalent Al/Ni and Ni/Al interfaces may be difficult to realize, leading to an uncontrolled energetic behavior of the overall multilayers. This basic understanding constitutes a crucial step to monitor the growth through specific Al and Ni (dual) deposition processes, further impacting initiation triggering and material stability. We also believe that these elementary and key chemical information will motivate further modeling investigations at the mesoscale to depict the overall extensions of Ni/Al and Al/Ni interfaces as a function of technological parameters, particularly the deposition temperatures, as suggested by the present work and reference.[13]

[1]F. Shimojo, A. Nakano, R. K. Kalia, and P. Vashishta, Appl. Phys. Lett. **95**, 043114 (2009).
[2]C. Rossi, K. Zhang, D. Esteve, P. Alphonse, P. Tailhades, and C. Vahlas, J. Microelectromech. Syst. **16**, 919 (2007).
[3]A. J. Gavens, D. Van Heerden, A. B. Mann, M. E. Reiss, and T. P. Weihs, J. Appl. Phys. **87**, 1255 (2000).
[4]K. J. Blobaum, M. E. Reiss, J. M. Plitzko-Lawrence, and T. P. Weihs, J. Appl. Phys. **94**, 5 (2003).
[5]Navid Amini Manesh, Saptarshi Basu, and Ranganathan Kumar, Combust. Flame **157**, 476 (2010).
[6]S. Zhao, T. C. Germann, and A. Strachan, J. Propul. Power **23**, 693 (2007).
[7]S. Zhao, T. C. Germann, and A. Strachan, J. Chem. Phys. **125**, 164707 (2006).
[8]Shijin Zhao, Timothy C. Germann, and Alejandro Strachan, Phys. Rev. B **76**, 104105 (2007).
[9]C. Kim and Y.-C. Chung, Jpn. J. Appl. Phys., Part 1 **44**, 5700 (2005).
[10]G. Kresse and D. Joubert, Phys. Rev. B **59**, 1758 (1999).
[11]D. Vanderbilt, Phys. Rev. B **41**, 7892 (1990).
[12]H. J. Monkhorst and J. D. Pack, Phys. Rev. B **13**, 5188 (1976).
[13]A. Hemeryck, M. Petrantoni, A. Esteve, C. Rossi, M. DjafariRouhani, G. Landa, and D. Esteve, J. Phys. Chem. Solids **71**, 125 (2010).